Jason J. Gorman
Benjamin Shapiro *Editors*

Feedback Control of MEMS to Atoms

Springer

Feedback Control of MEMS to Atoms

Jason J. Gorman • Benjamin Shapiro
Editors

Feedback Control of MEMS to Atoms

Springer

Editors
Jason J. Gorman
National Institute of Standards
& Technology (NIST)
Intelligent Systems Division
100 Bureau Drive
Stop 8230 Gaithersburg
MD 20899
USA
gorman@nist.gov

Benjamin Shapiro
University of Maryland
2330 Kim Building
College Park
MD 20742
USA
benshap@umd.edu

ISBN 978-1-4419-5831-0 e-ISBN 978-1-4419-5832-7
DOI 10.1007/978-1-4419-5832-7
Springer New York Dordrecht Heidelberg London

Library of Congress Control Number: 2011937573

Preface

This book explores the control of systems on small length scales. Research and development for micro- and nanoscale science and technology has grown quickly over the last decade, particularly in the areas of microelectromechanical systems (MEMS), microfluidics, nanoelectronics, bio-nanotechnologies, nanofabrication, and nanomaterials. However, to date, control theory has played only a small role in the advancement of this research. As we know from the technical progression of macroscale intelligent systems, such as assembly robots and fly-by-wire aircraft, control systems can maximize system performance and, in many cases, enable capabilities that would otherwise not be possible. We expect that control systems will play a similar enabling role in the development of the next generation of micro- and nanoscale devices, as well as in the precision instrumentation that will be used to fabricate and measure these devices. In support of this, each chapter of this book provides an introduction to an application of micro- and nanotechnologies in which control systems have already been shown to be critical to its success. Through these examples, we aim to provide insight into the unique challenges in controlling systems at small length scales and to highlight the benefits in merging control systems and micro- and nanotechnologies.

We conceived of this book because we saw a strong need to bring the control systems and micro- and nanosystems communities closer together. In our view, the intersection between these two groups is still very small, impeding the advancement of active, precise, and robust micro- and nanoscale systems that can meet the demanding requirements for commercial, military, medical, and consumer products. As an example, we attend conferences for both the control systems and micro- and nanoscale science and technology communities and have found the overlap between attendees to be marginal; maybe in the tens of people. Our hope is that this book will be a step toward rectifying this situation by bridging the gap between these two communities and demonstrating that concrete benefits for both fields can be achieved through collaborative research. We also hope to motivate the next generation of young engineers and scientists to pursue a career at this intersection, which offers all of the excitement, frustration, and eventual big rewards that an aspiring researcher could want.

This book is targeted toward both control systems researchers interested in pursuing new application in the micro- and nanoscales domains, and researchers developing micro- and nanosystems who are interested in learning how control systems can benefit their work. For the former, we hope these chapters will show the serious effort required to demonstrate control in a new application area. All of the contributing authors have acquired expertise in at least one new scientific area in addition to control theory (e.g., atomic force microscopy, optics, microfluidics) in order to pursue their area of research. Acquiring dual expertise can take years of effort, but the payoff can be high by providing results that no expert in a single domain can accomplish. Additionally, it can result in fascinating work (we hope some of the challenges and excitement are conveyed). For researchers in micro- and nanoscale science and technology, this book contains concrete examples of the benefits that control can provide. These range from better control of particle size distribution during synthesis, to high-bandwidth and reliable nanoscale positioning and imaging of objects, to optimal control of the spin dynamics of quantum systems. We also hope this book will be of use to those who are not yet experts in either control systems or micro- and nanoscale systems but are interested in both. We believe it will provide a useful and instructive introduction to the breadth of research being performed at the intersection of these two fields.

The topics covered in this book were selected to represent the entire length scale of miniaturized systems, ranging from hundreds of micrometers down to a fraction of a nanometer (hence our title, *Feedback Control of MEMS to Atoms*). They were also selected to cover a broad range of physical systems that will likely provide new material to most readers.

Acknowledgments We would like to express our deepest appreciation to all of the researchers who contributed to this book. Without them this project would not have been possible. It was a pleasure to have the opportunity to work with them. We would also like to thank the staff at Springer and in particular, Steven Elliot, who provided us with outstanding guidance and motivation throughout the process.

Gaithersburg Jason J. Gorman
College Park Benjamin Shapiro

Contents

Chapter 1
Introduction

Jason J. Gorman and Benjamin Shapiro

The goal of this book is to illustrate how control tools can be successfully applied to micro- and nano-scale systems. The book partially explores the wide variety of applications where control can have a significant impact at the micro- and nanoscale, and identifies key challenges and common approaches. This first chapter briefly outlines the range of subjects within micro and nano control and introduces topics that recur throughout the book.

1.1 Controlling Micro- and Nanoscale Systems

Microelectromechanical systems (MEMS) emerged, at the beginning of the 1980s, as a cost effective and highly sensitive solution for many sensor applications, including pressure, force, and acceleration measurements. Since then, MEMS has grown into a $6 billion industry and a number of other microtechnologies have followed, including microfluidics, microrobotics, and micromachining. Simultaneously, nanotechnology has become one of the largest areas of scientific and engineering research, with over $12 billion invested over the last decade by the U.S. Government alone. This research has resulted in a new set of materials and devices that offer unique physical and chemical properties due to their nanoscale dimensions, which are expected to yield better products and services.

J.J. Gorman (✉)
Intelligent Systems Division, Engineering Laboratory, National Institute of Standards and Technology, Gaithersburg, MD 20899, USA
e-mail: gorman@nist.gov

B. Shapiro
Fischell Department of Bioengineering, Institute for Systems Research (ISR), University of Maryland, College Park, MD 20742, USA
e-mail: benshap@umd.edu

J.J. Gorman and B. Shapiro (eds.), *Feedback Control of MEMS to Atoms*,
DOI 10.1007/978-1-4419-5832-7_1, © Springer Science+Business Media, LLC 2012

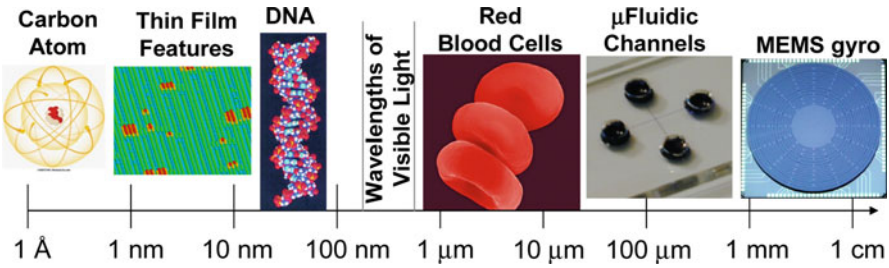

Fig. 1.1 A sense of scale: the sizes of things from a single carbon atom to an integrated MEMS gyro (Images used with permission. Copyrights Denis Kunkel Microscopy, Inc. and Springer)

Micro- and nanotechnology integrated systems refer to a combination of components that provide enhanced functionality that would not be possible with each component alone. Familiar examples of systems at the macroscale include robots, aircraft, automobiles, and information networks, where each system is composed of actuators, sensors, and computational logic that allow for complex and controlled behavior. Micro- and nano-systems only differ from their macroscale counterparts in that essential system behavior occurs at minute length scales. In some cases, micro- and nanosystems are large in size but are dependent on micro- or nanoscale phenomena (e.g., a scanning probe microscope), whereas in other cases the entire system is miniaturized (e.g., a MEMS accelerometer). Other examples of micro- and nanosystems include nanomechanical resonators, cell micromanipulators, and nanofabrication tools. Clearly this is a diverse group of systems, but as will be seen in this book, there are a variety of common threads for the integration and control of such systems, as well as common principles to address these threads.

Feedback control is necessary at small length scales for the same reasons that it is needed in macroscale applications: to correct for errors in system variables in real-time to improve performance, to provide robust operation in the face of unknown or uncertain conditions, and to enable new system capabilities. This book explores emerging efforts to apply control systems to micro- and nanoscale systems in order to realize these benefits and, as a result, accelerate the utility and adoption of these technologies.

Going down in length scales, to micrometers and nanometers (Fig. 1.1), opens up a wide set of technologies, opportunities, and challenges. Sensors and actuators at small scales can directly access and manipulate microscopic and nanoscopic objects, and are thus being used to study surfaces with atomic resolution and to process individual cells. The associated system tasks are new (e.g., manipulate nanoscopic objects), there are additional physical effects to be considered and understood (e.g., molecule to molecule interactions and atomic spins), and previously small phenomena can now dominate (e.g., surface effects, like surface tension, now surpass bulk phenomena, like gravity or momentum). Thus system control techniques

must be modified or newly developed, as must the modeling, sensing, actuation, and real-time computation that supports them. As a result, the merging of control systems with micro- and nanoscale systems represents a new field that we expect to grow considerably over the coming decade. The intention of this book is to provide an introductory survey.

1.2 Critical Application Areas

There is a lot of diversity in the micro and nanoscale systems where control is playing a role. However, the majority of the applications fit within at least one of the five following groups: micro- and nanomanufacturing, instruments for nanoscale research, MEMS/NEMS, micro/nanofluidics, and quantum systems. This taxonomy has influenced the structure of this book and provides a starting point for finding the most important applications to pursue. Some of the applications and devices where control can play an important role are listed below. Only a small percentage of these applications have seen a concerted control implementation research effort. Therefore, there remain considerable opportunities for control practitioners to make important contributions to this field in the near and long term.

Micro- and Nanomanufacturing: Nanolithography including scanning probe and nanoimprint techniques, micro- and nanoassembly, directed self-assembly, nanoscale material deposition processes, nanoparticle growth, and formation of composite nanomaterials.

Instruments for Nanoscale Research: Scanning probe microscopy including atomic force microscopy, scanning tunneling microscopy, and near-field scanning optical microscopy. Particle trapping includes optical and magnetic trapping, particle tracking and localization.

MEMS/NEMS: MEMS/NEMS (micro/nano-electro-mechanical-systems) including inertial devices such as accelerometers and gyroscopes; micromirrors and other optomechanical components; filters, switches, and resonators for radiofrequency (RF) communications; probe-based data storage and hard drive read heads; biochemical sensors for medical diagnostics and threat detection; and micro- and nanorobots.

Micro/Nanofluidics: Micro/Nanofluidics include lab-on-a-chip technologies, inexpensive medical diagnostics, embedded drug delivery systems, and inkjet valves for high-volume printing.

Quantum Systems: Quantum systems include quantum computing, quantum communication and encryption, nuclear magnetic resonance imaging, and atom trapping and cooling.

1.3 Overview of the Chapters

The contributors to this book were chosen because they are leaders in their respective research areas and have either been able to demonstrate significant experimental results, or are well on their way towards experiments. It can take a long time to get from an initial control concept to an experimental demonstration: all the chosen contributors have been working on control of small systems for at least 5 to 10 years. Given that the field of micro/nanoscale systems is itself still fairly new (30+ years in the case of MEMS) and that there was a delay between the inception of the field and the subsequent entry of control researchers, in this sense, these contributors are at the leading edge. Of course, we could not include every major researcher at the intersection of controls and micro- and nanosystems, but we believe that we have chosen a representative sampling across a diverse set of applications that demonstrate how control is beginning to be applied on small length scales. We expect that there will be many more researchers in the future with many more exciting, and needed, applications and results.

The chapters have been organized along the lines of the application areas listed in the previous section: micro/nanomanufacturing, instruments for nanoscale research, MEMS, microfluidics, and quantum systems. Chapters 2 to 4 explore controlled manufacturing. Control of nanoparticle size during synthesis is presented in Chap. 2, and Chap. 3 discusses the estimation of nanoscale surface properties during manufacturing using optical measurements and Kalman filtering techniques. Automated assembly of two-dimensional structures composed of micro- and nanoparticles is presented in Chap. 4. The control of instruments for nanoscale research is discussed in Chaps. 5 and 6. Improving the imaging performance of atomic force microscopes using robust control is covered in Chap. 5 and the control of optically trapped particles is discussed in Chap. 6. The control of MEMS and microfluidic systems is the subject of Chaps. 7 through 9. Position control of MEMS actuators is presented in Chap. 7, closed-loop operation of precision MEMS gyroscopes is covered in Chap. 8, and the control of particle motion within a microfluidic system is presented in Chap. 9. Finally, quantum control is presented in Chap. 10 with an emphasis on controlling spin dynamics in quantum mechanical systems. In the final chapter, a review of some of the common challenges encountered throughout the book is presented along with prospects for future research in controlling micro- and nanoscale systems.

1.4 Notes for the Reader

This book was written for scientists and engineers in the fields of both micro/nanotechnologies and control systems with the intention of bridging the gap between the two. For the former group, it shows how control is being applied

to miniaturized systems and highlights the benefits of feedback control for these systems. There is also an emphasis on the importance of interdisciplinary collaboration, physical modeling, control design mathematics, and experimentation in realizing these benefits. For the latter group, it provides an introduction to how control is currently being applied, extended, and developed for miniaturized systems. It also documents the need to fully understand the capabilities, requirements, and bottlenecks in new application areas before approaching the control design problem. It is our intention that this book provide an impetus for each group to better learn the technical language of the other – a requirement for successful collaboration between the two. But above all, our greatest hope is that it will spark new ideas and insights to enable better interactions between these two fields and result in significant advances in micro- and nanoscale systems.

Due to the multidisciplinary nature of this book, some background reading may be helpful. Readers who are not familiar with control theory can find an introduction written for a broad audience in [1] and practical 'fast-track' advice for implementing linear feedback controllers in [2]. More rigorous treatments of control theory are found in [3], a concise book that crucially describes not only what control can achieve for any given system but also what it cannot. Control theory is usually introduced in a linear system setting, where strong and comprehensive results are available, but there are also more advanced books that deal with control for nonlinear systems [4]. Nonlinear methods require a higher level of mathematical sophistication, but are needed in many real-world situations where nonlinearities cannot be neglected, as seen in several chapters in this book.

Readers not familiar with micro- and nanoscale systems can find an excellent introduction to microelectromechanical systems (MEMS) in [5–7]. The first of these reference includes, as its first chapter, the classic 1959 Feynman lecture 'There is Plenty of Room at the Bottom' [8]. There are also a number of books that introduce nanoscale science (e.g., [9, 10]) and nanotechnology [11, 12]. Texts relevant to the physics of micro- and nanoscale systems span the spectrum from optics and electronics to mechanics, fluid dynamics, and chemistry and biology. When faced with diving into a new field of physics and learning the basics, the Feynman lectures [13] are a fantastic resource. Each lecture provides a brilliant, concise, and accurate introduction to an entire field.

Finally, for both the controls and micro/nanoreaders, four fairly recent reports provide context for how control methods apply to novel systems in the areas of atomic force microscopy and nanorobotic manipulation [14]: MEMS, biological, chemical, and nanoscale systems [15, 16]; and networks of large and small systems, including aerospace, transportation, information technology, robotics, biology, medicine, and materials [17]. Many of the recommendations made in these reports are mirrored in the research and approaches described in this book.

References

1. R.M. Murray and K.J. Åström, *Feedback systems: An introduction for scientists and engineers*, Princeton University Press, Princeton, NJ, 2008.
2. A. Abramovici and J. Chapsky. *Feedback control systems: A fast-track guide for scientists and engineerings*, Kluwer, Norwell, MA, 2000.
3. J.C. Doyle, B.A. Francis, and A.R. Tannenbaum. *Feedback control theory*, Macmillan, New York, 1992.
4. A. Isidori. *Nonlinear control systems*, Springer, London, 1995.
5. W.S. Trimmer (editor). *Micromechanics and MEMS: Classic and seminal papers to 1990*, IEEE Press, New York, 1997.
6. N. Maluf. *An introduction to microelectromechanical systems engineering*, Artech House, Boston, MA, 2000.
7. C. Liu. *Foundations of MEMS*, Prentice-Hall, Englewood Cliffs, NJ, 2011.
8. R. Feynman. *There's plenty of room at the bottom. Caltech engineering and science magazine*, 23, 1960.
9. E.L. Wolf. *Nanophysics and nanotechnology: An introduction to modern concepts in nanoscience*, Wiley, Weinheim, Germany, 2006.
10. S. Lindsay. *Introduction to nanoscience*, Oxford University Press, New York, 2009.
11. B. Bhushan. *Springer handbook of nanotechnology*, Springer, New York, 2010.
12. A. Busnaina. *Nanomanufacturing handbook*, CRC Press, Boca Raton, FL, 2006.
13. R.P. Feynman, R.B. Leighton, and M. Sands. *The Feynman lectures on physics*, Addison-Wesley, Boston, MA , 1964.
14. M. Sitti. *NSF workshop on future directions in nano-scale systems, dynamics and control*, final report, 2003.
15. B. Shapiro. *NSF workshop on control and system integration of micro- and nano-scale systems*, final report, 2004. Available: http://www.isr.umd.edu/CMN-NSFwkshp/.
16. B. Shapiro. Workshop on control of micro- and nano-scale systems, *IEEE control systems magazine*, 25:82–88, 2005.
17. R.M. Murray (editor). *Control in an information rich world: Report of the panel on future directions in control, dynamics, and systems*. SIAM, Philadelphia, PA. 2003. Available: http://www.cds.caltech.edu/~murray/cdspanel.

Chapter 2
Feedback Control of Particle Size Distribution in Nanoparticle Synthesis and Processing

Mingheng Li and Panagiotis D. Christofides

2.1 Introduction

Particulate processes (also known as dispersed-phase processes) are characterized by the co-presence of and strong interaction between a continuous (gas or liquid) phase and a particulate (dispersed) phase and are essential in making many high-value industrial products. Particulate processes play a prominent role in a number of process industries since about 60% of the products in the chemical industry are manufactured as particulates with an additional 20% using powders as ingredients. Representative examples of particulate processes for micro- and nano-particle synthesis and processing include the crystallization of proteins for pharmaceutical applications [2], the emulsion polymerization of nano-sized latex particles [50], the aerosol synthesis of nanocrystalline catalysts [64], and thermal spray processing of nanostructured functional thermal barrier coatings to protect turbine blades [1]. The industrial importance of particulate processes and the realization that the physicochemical and mechanical properties of materials made with particulates depend heavily on the characteristics of the underlying particle-size distribution (PSD) have motivated significant research attention over the last ten years on model-based control of particulate processes. These efforts have also been complemented by recent and ongoing developments in measurement technology which allow the accurate and fast online measurement of key process variables including important characteristics of PSDs (e.g., [37,55,56]). The recent efforts on model-based control

M. Li (✉)
Department of Chemical and Materials Engineering, California State Polytechnic University, Pomona, CA 91768, USA
e-mail: minghengli@csupomona.edu

P.D. Christofides
Department of Chemical and Biomolecular Engineering, University of California, Los Angeles, CA 90095, USA
e-mail: pdc@seas.ucla.edu

J.J. Gorman and B. Shapiro (eds.), *Feedback Control of MEMS to Atoms*,
DOI 10.1007/978-1-4419-5832-7_2,

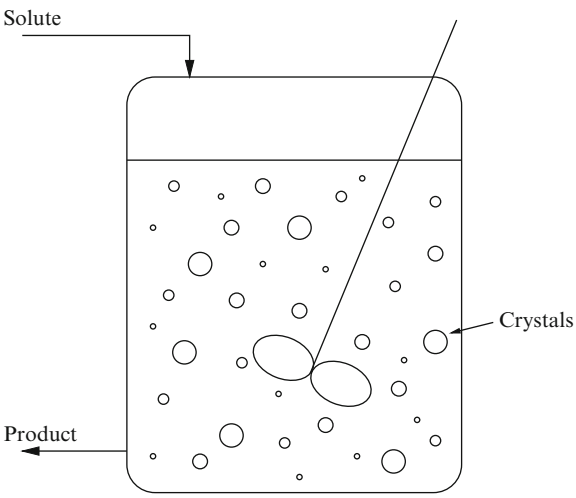

Fig. 2.1 Schematic of a continuous crystallizer

of particulate processes have also been motivated by significant advances in the physical modeling of highly coupled reaction-transport phenomena in particulate processes that cannot be easily captured through empirical modeling. Specifically, population balances have provided a natural framework for the mathematical modeling of PSDs in broad classes of particulate processes (see, for example, the tutorial article [30] and the review article [54]), and have been successfully used to describe PSDs in emulsion polymerization reactors (e.g., [13, 15]), crystallizers (e.g., [4, 55]), aerosol reactors (e.g., [23]), and cell cultures (e.g., [12]). To illustrate the structure of the mathematical models that arise in the modeling and control of particulate processes, we focus on three representative examples: continuous crystallization, batch crystallization, and aerosol synthesis.

2.1.1 Continuous Crystallization

Crystallization is a particulate process, which is widely used in industry for the production of many micro- or nano-sized products including fertilizers, proteins, and pesticides. A typical continuous crystallization process is shown in Fig. 2.1. Under the assumptions of isothermal operation, constant volume, well-mixed suspension, nucleation of crystals of infinitesimal size and mixed product removal, a dynamic model for the crystallizer can be derived from a population balance for the particle phase and a mass balance for the solute concentration and has the following mathematical form [32, 39]:

$$\begin{aligned}\frac{\partial n(r,t)}{\partial t} &= -\frac{\partial (R(t)n(r,t))}{\partial r} - \frac{n(r,t)}{\tau} + \delta(r-0)Q(t),\\ \frac{\mathrm{d}c(t)}{\mathrm{d}t} &= \frac{(c_0-\rho)}{\varepsilon(t)\tau} + \frac{(\rho-c(t))}{\tau} + \frac{(\rho-c(t))}{\varepsilon(t)}\frac{\mathrm{d}\varepsilon(t)}{\mathrm{d}t},\end{aligned} \tag{2.1}$$

where $n(r,t)dr$ is the number of crystals in the size range of $[r, r+dr]$ at time t per unit volume of suspension, τ is the residence time, ρ is the density of the crystal, $c(t)$ is the solute concentration in the crystallizer, c_0 is the solute concentration in the feed, and

$$\varepsilon(t) = 1 - \int_0^\infty n(r,t)\frac{4}{3}\pi r^3 \mathrm{d}r$$

is the volume of liquid per unit volume of suspension. $R(t)$ is the crystal growth rate, $\delta(r-0)$ is the standard Dirac function, and $Q(t)$ is the crystal nucleation rate. The term $\delta(r-0)Q(t)$ accounts for the production of crystals of infinitesimal (zero) size via nucleation. An example of expressions of $R(t)$ and $Q(t)$ is the following:

$$R(t) = k_1(c(t) - c_s), \quad Q(t) = \varepsilon(t)k_2 \mathrm{e}^{-\frac{k_3}{(c(t)/c_s - 1)^2}}, \tag{2.2}$$

where k_1, k_2, and k_3 are constants and c_s is the concentration of solute at saturation. For a variety of operating conditions (see [6] for model parameters and detailed studies), the continuous crystallizer model of (2.1) exhibits highly oscillatory behavior (the main reason for this behavior is that the nucleation rate is much more sensitive to supersaturation relative to the growth rate – i.e., compare the dependence of $R(t)$ and $Q(t)$ on the values of $c(t)$ and c_s), which suggests the use of feedback control to ensure stable operation and attain a crystal size distribution (CSD) with desired characteristics. To achieve this control objective, the inlet solute concentration can be used as the manipulated input and the crystal concentration as the controlled and measured output.

2.1.2 Batch Protein Crystallization

Batch crystallization plays an important role in the pharmaceutical industry. We consider a batch crystallizer, which is used to produce tetragonal HEW (hen-egg-white) lysozyme crystals from a supersaturated solution [62]. A schematic of the batch crystallizer is shown in Fig. 2.2. Applying population, mass and energy balances to the process, the following mathematical model is obtained:

$$\begin{aligned}
&\frac{\partial n(r,t)}{\partial t} + G(t)\frac{\partial n(r,t)}{\partial r} = 0, \quad n(0,t) = \frac{B(t)}{G(t)},\\
&\frac{\mathrm{d}C(t)}{\mathrm{d}t} = -24\rho k_v G(t)\mu_2(t),\\
&\frac{\mathrm{d}T(t)}{\mathrm{d}t} = -\frac{UA}{MC_\mathrm{p}}(T(t) - T_j(t)),
\end{aligned} \tag{2.3}$$

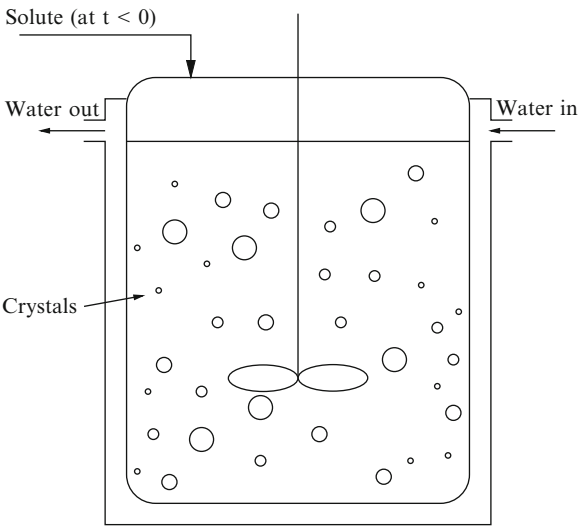

Fig. 2.2 Schematic of a batch cooling crystallizer

where $n(r,t)$ is the CSD, $B(t)$ is the nucleation rate, $G(t)$ is the growth rate, $C(t)$ is the solute concentration, $T(t)$ is the crystallizer temperature, $T_j(t)$ is the jacket temperature, ρ is the density of crystals, k_v is the volumetric shape factor, U is the overall heat-transfer coefficient, A is the total heat-transfer surface area, M is the mass of solvent in the crystallizer, C_p is the heat capacity of the solution, and $\mu_2(t) = \int_0^\infty r^2 n(r,t)\mathrm{d}r$ is the second moment of the CSD. The nucleation rate, $B(t)$, and the growth rate, $G(t)$, are given by [62]:

$$B(t) = k_a C(t) \exp\left(-\frac{k_b}{\sigma^2(t)}\right), \; G(t) = k_g \sigma^g(t), \tag{2.4}$$

where $\sigma(t)$, the supersaturation, is a dimensionless variable and is defined as $\sigma(t) = \ln(C(t)/C_s(T(t)))$, $C(t)$ is the solute concentration, g is the exponent relating growth rate to the supersaturation, and $C_s(T)$ is the saturation concentration of the solute, which is a nonlinear function of the temperature of the form:

$$C_s(T) = 1.0036 \times 10^{-3} T^3 + 1.4059 \times 10^{-2} T^2 - 0.12835T + 3.4613. \tag{2.5}$$

The existing experimental results [68] show that the growth condition of tetragonal HEW lysozyme crystal is significantly affected by the supersaturation. Low supersaturation will lead to the cessation of the crystal growth. On the other hand, rather than forming tetragonal crystals, large amount of needle crystals will form when the supersaturation is too high. Therefore, a proper range of supersaturation is necessary to guarantee the product's quality. The jacket temperature, T_j, is manipulated to achieve the desired crystal shape and size distribution.

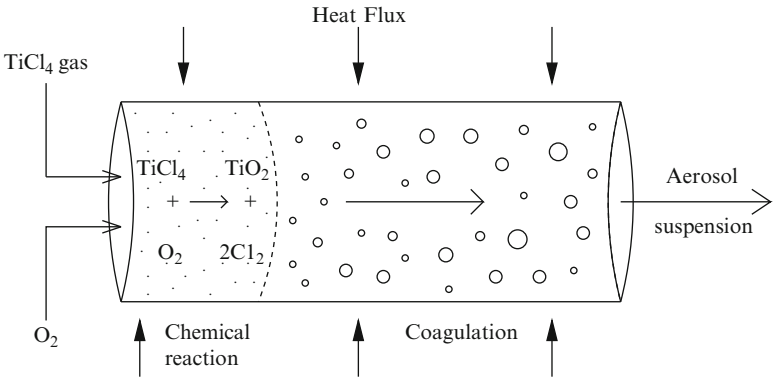

Fig. 2.3 Schematic of a titania aerosol reactor

2.1.3 Aerosol Synthesis

Aerosol processes are increasingly being used for the large-scale production of nano- and micron-sized particles. A typical aerosol flow reactor for the synthesis of titania aerosol with simultaneous chemical reaction, nucleation, condensation, coagulation, and convective transport is shown in Fig. 2.3. A general mathematical model, which describes the spatiotemporal evolution of the particle size distribution in such aerosol processes can be obtained from a population balance and consists of the following nonlinear partial integro-differential equation [33, 34]:

$$\frac{\partial n(v,z,t)}{\partial t} + v_z \frac{\partial n(v,z,t)}{\partial z} + \frac{\partial (G(\bar{x},v,z)n(v,z,t))}{\partial v} - I(v^*)\delta(v-v^*)$$
$$= \frac{1}{2}\int_0^v \beta(v-\bar{v},\bar{v},\bar{x})n(v-\bar{v},t)n(\bar{v},z,t)\mathrm{d}\bar{v} - n(v,z,t)\int_0^\infty \beta(v,\bar{v},\bar{x})n(\bar{v},z,t)\mathrm{d}\bar{v}, \quad (2.6)$$

where $n(v,z,t)$ denotes the particle size distribution function, v is the particle volume, t is the time, $z \in [0,L]$ is the spatial coordinate, L is the length scale of the process, v^* is the size of the nucleated aerosol particles, v_z is the velocity of the fluid, $\bar{x}$ is the vector of the state variables of the continuous phase, $G(\cdot,\cdot,\cdot), I(\cdot), \beta(\cdot,\cdot,\cdot)$ are nonlinear scalar functions which represent the growth, nucleation, and coagulation rates and $\delta(\cdot)$ is the standard Dirac function. The model of (2.6) is coupled with a mathematical model, which describes the spatiotemporal evolution of the concentrations of species and temperature of the gas phase $(\bar{x})$ that can be obtained from mass and energy balances. The control problem is to regulate process variables such as inlet flow rates and wall temperature to produce aerosol products with desired size distribution characteristics.

The mathematical models of (2.1), (2.3) and (2.6) demonstrate that particulate process models are nonlinear and distributed parameter in nature. These properties have motivated extensive research on the development of efficient numerical

methods for the accurate computation of their solution (see, for example, [12, 23, 25, 38, 48, 54, 63]). However, in spite of the rich literature on population balance modeling, numerical solution, and dynamical analysis of particulate processes, up to about ten years ago, research on model-based control of particulate processes had been very limited. Specifically, early research efforts had mainly focused on the understanding of fundamental control-theoretic properties (controllability and observability) of population balance models [58] and the application of conventional control schemes (such as proportional-integral and proportional-integral-derivative control, self-tuning control) to crystallizers and emulsion polymerization processes (see, for example, [13, 57, 59] and the references therein). The main difficulty in synthesizing nonlinear model-based feedback controllers for particulate processes is the distributed parameter nature of the population balance models, which does not allow their direct use for the synthesis of low-order (and therefore, practically implementable) model-based feedback controllers. Furthermore, a direct application of the aforementioned solution methods to particulate process models leads to finite dimensional approximations of the population balance models (i.e., nonlinear ordinary differential equation (ODE) systems in time) which are of very high order, and thus inappropriate for the synthesis of model-based feedback controllers that can be implemented in realtime. This limitation had been the bottleneck for model-based synthesis and real-time implementation of model-based feedback controllers on particulate processes.

2.2 Model-Based Control of Particulate Processes

2.2.1 Overview

Motivated by the lack of population balance-based control methods for particulate processes and the need to achieve tight size distribution control in many particulate processes, we developed, over the last ten years, a general framework for the synthesis of nonlinear, robust, and predictive controllers for particulate processes based on population balance models [6–9, 16, 33, 35, 60, 62]. Specifically, within the developed framework, nonlinear low-order approximations of the particulate process models are initially derived using order reduction techniques and are used for controller synthesis. Subsequently, the infinite-dimensional closed-loop system stability, performance and robustness properties were precisely characterized in terms of the accuracy of the approximation of the low-order models. Furthermore, controller designs were proposed that deal directly with the key practical issues of uncertainty in model parameters, unmodeled actuator/sensor dynamics and constraints in the capacity of control actuators and the magnitude of the process state variables. It is also important to note that owing to the low-dimensional structure of the controllers, the computation of the control action involves the solution of a small set of ODEs, and thus, the developed controllers can be readily

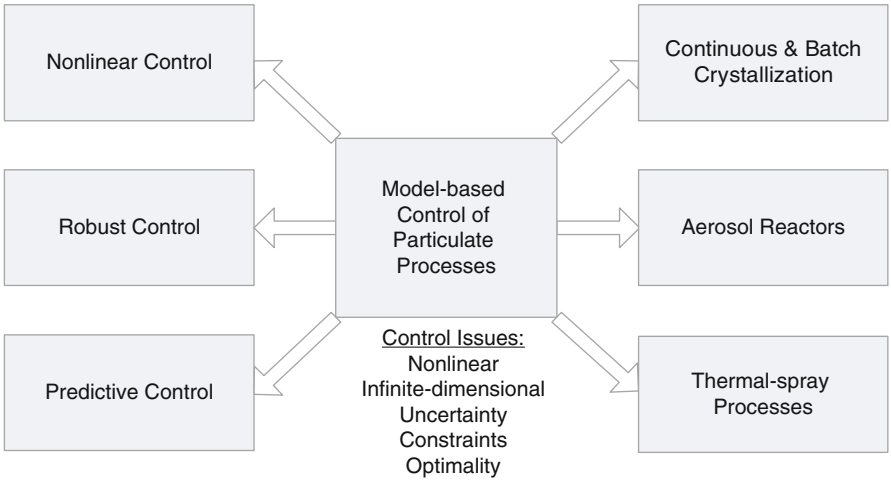

Fig. 2.4 Summary of our research on model-based control of particulate processes

implemented in realtime with reasonable computing power, thereby resolving the main issue on model-based control of particulate processes. In addition to theoretical developments, we also successfully demonstrated the application of the proposed methods to size distribution control in continuous and batch crystallization, aerosol, and thermal spray processes and documented their effectiveness and advantages with respect to conventional control methods. Figure 2.4 summarizes these efforts. The reader may refer to [4, 12, 15] for recent reviews of results on simulation and control of particulate processes.

2.2.2 Particulate Process Model

To present the main elements of our approach to model-based control of particulate processes, we focus on a general class of spatially homogeneous particulate processes with simultaneous particle growth, nucleation, agglomeration, and breakage. Examples of such processes have been introduced in the previous section. Assuming that particle size is the only internal particle coordinate and applying a dynamic material balance on the number of particles of size r to $r+dr$ (population balance), we obtain the following general nonlinear partial integro-differential equation, which describes the rate of change of the PSD, $n(r,t)$:

$$\frac{\partial n}{\partial t} = -\frac{\partial (G(x,r)n)}{\partial r} + w(n,x,r), \tag{2.7}$$

where $n(r,t)$ is the particle number size distribution, $r \in [0, r_{\max}]$ is the particle size, and $r_{\max}$ is the maximum particle size (which may be infinity), t is the time and

$x \in \mathbb{R}^n$ is the vector of state variables, which describe properties of the continuous phase (for example, solute concentration, temperature, and pH in a crystallizer); see (2.8) for the system that describes the dynamics of x. $G(x,r)$ and $w(n,x,r)$ are nonlinear scalar functions whose physical meaning can be explained as follows: $G(x,r)$ accounts for particle growth through condensation and is usually referred to as growth rate. It usually depends on the concentrations of the various species present in the continuous phase, the temperature of the process, and the particle size. On the other hand, $w(n,x,r)$ represents the net rate of introduction of new particles into the system. It includes all the means by which particles appear or disappear within the system including particle agglomeration (merging of two particles into one), breakage (division of one particle to two) as well as nucleation of particles of size $r \geq 0$ and particle feed and removal. The rate of change of the continuous-phase variables x can be derived by a direct application of mass and energy balances to the continuous phase and is given by a nonlinear integro-differential equation system of the general form:

$$\dot{x} = f(x) + g(x)u(t) + A\int_0^{r_{\max}} a(n,r,x)\mathrm{d}r, \tag{2.8}$$

where $f(x)$ and $a(n,r,x)$ are nonlinear vector functions, $g(x)$ is a nonlinear matrix function, A is a constant matrix and $u(t) = [u_1\ u_2\ \cdots\ u_m] \in \mathbb{R}^m$ is the vector of manipulated inputs. The term $A\int_0^{r_{\max}} a(n,r,x)\mathrm{d}r$ accounts for mass and heat transfer from the continuous phase to all the particles in the population (see [8] for details).

2.2.3 Model Reduction of Particulate Process Models

While the population balance models are infinite dimensional systems, the dominant dynamic behavior of many particulate process models has been shown to be low dimensional. Manifestations of this fundamental property include the occurrence of oscillatory behavior in continuous crystallizers [32] and the ability to capture the long-term behavior of aerosol systems with self-similar solutions [23]. Motivated by this, we introduced a general methodology for deriving low-order ODE systems that accurately reproduce the dominant dynamics of the nonlinear integro-differential equation system of (2.7) and (2.8) [6]. The proposed model reduction methodology exploits the low-dimensional behavior of the dominant dynamics of the system of (2.7) and (2.8) and is based on a combination of the method of weighted residuals with the concept of approximate inertial manifolds.

Specifically, the proposed approach initially employs the method of weighted residuals (see [54] for a comprehensive review of results on the use of this method for solving population balance equations) to construct a nonlinear, possibly high-order, ODE system that accurately reproduces the solutions and dynamics of the distributed parameter system of (2.7) and (2.8). We first consider an orthogonal

set of basis functions $\phi_k(r)$, where $r \in [0, r_{\max})$, $k = 1, \ldots, \infty$, and expand the particle size distribution function $n(r,t)$ in an infinite series in terms of $\phi_k(r)$ as follows:

$$n(r,t) = \sum_{k=1}^{\infty} a_k(t)\phi_k(r), \tag{2.9}$$

where $a_k(t)$ are time-varying coefficients. In order to approximate the system of (2.7) and (2.8) with a finite set of ODEs, we obtain a set of N equations by substituting (2.9) into (2.7) and (2.8), multiplying the population balance with N different weighting functions $\psi_\nu(r)$ (that is, $\nu = 1, \ldots, N$), and integrating over the entire particle size spectrum. In order to obtain a finite dimensional model, the series expansion of $n(r,t)$ is truncated up to order N. The infinite dimensional system of (2.7) reduces to the following finite set of ODEs:

$$\begin{aligned}
&\int_0^{r_{\max}} \psi_\nu(r) \sum_{k=1}^{N} \phi_k(r) \frac{\partial a_{kN}(t)}{\partial t} \mathrm{d}r = \sum_{k=1}^{N} a_{kN}(t) \int_0^{r_{\max}} \psi_\nu(r) \frac{\partial (G(x_N, r)\phi_k(r))}{\partial r} \mathrm{d}r, \\
&\quad + \int_0^{r_{\max}} \psi_\nu(r) w\left(\sum_{k=1}^{N} a_{kN}(t)\phi_k(r), x_N, r \right) \mathrm{d}r, \ \nu = 1, \ldots, N \\
&\dot{x}_N = f(x_N) + g(x_N)u(t) + A \int_0^{r_{\max}} a\left(\sum_{k=1}^{N} a_{kN}(t)\phi_k(r), r, x_N \right) \mathrm{d}r,
\end{aligned} \tag{2.10}$$

where x_N and a_{kN} are the approximations of x and a_k obtained by an N-th order truncation. From (2.10), it is clear that the form of the ODEs that describe the rate of change of $a_{kN}(t)$ depends on the choice of the basis and weighting functions, as well as on N. The system of (2.10) was obtained from a direct application of the method of weighted residuals (with arbitrary basis functions) to the system of (2.7) and (2.8), and thus, may be of very high order in order to provide an accurate description of the dominant dynamics of the particulate process model. High-dimensionality of the system of (2.10) leads to complex controller design and high-order controllers, which cannot be readily implemented in practice. To circumvent these problems, we exploited the low-dimensional behavior of the dominant dynamics of particulate processes and proposed an approach based on the concept of inertial manifolds to derive low-order ODE systems that accurately describe the dominant dynamics of the system of (2.10) [6]. This order reduction technique initially employs singular perturbation techniques to construct nonlinear approximations of the modes neglected in the derivation of the finite dimensional model of (2.10) (i.e., modes of order $N+1$ and higher) in terms of the first N modes. Subsequently, these steady-state expressions for the modes of order $N+1$ and higher (truncated up to appropriate order) are used in the model of (2.10) (instead of setting them to zero) and significantly improve the accuracy of the model of (2.10) without increasing its dimension; details on this procedure can be found in [6].

It is important to note that the method of weighted residuals reduces to the method of moments when the basis functions are chosen to be Laguerre polynomials

and the weighting functions are chosen as $\psi_\nu = r^\nu$. The moments of the particle size distribution are defined as:

$$\mu_\nu = \int_0^\infty r^\nu n(r,t)\mathrm{d}r, \quad \nu = 0,\ldots,\infty \tag{2.11}$$

and the moment equations can be directly generated from the population balance model by multiplying it by r^ν, $\nu = 0,\ldots,\infty$ and integrating from 0 to ∞. The procedure of forming moments of the population balance equation very often leads to terms that may not reduce to moments, terms that include fractional moments, or to an unclosed set of moment equations. To overcome this problem, the particle size distribution may be expanded in terms of Laguerre polynomials defined in $L_2[0,\infty)$ and the series solution using a finite number of terms may be used to close the set of moment equations (this procedure has been successfully used for models of crystallizers with fine traps used to remove small crystals [7]).

2.2.4 Model-Based Control Using Low-Order Models

2.2.4.1 Nonlinear Control

Low-order models can be constructed using the techniques described in the previous section. We describe an application to the continuous crystallization process of Sect. 2.1.1. First, the method of moments is used to derive the following infinite-order dimensionless system from (2.1) for the continuous crystallization process:

$$\begin{aligned}
\frac{\mathrm{d}\tilde{x}_0}{\mathrm{d}t} &= -\tilde{x}_0 + (1-\tilde{x}_3)Da\mathrm{e}^{-F/\tilde{y}^2},\\
\frac{\mathrm{d}\tilde{x}_1}{\mathrm{d}t} &= -\tilde{x}_1 + \tilde{y}\tilde{x}_0,\\
\frac{\mathrm{d}\tilde{x}_2}{\mathrm{d}t} &= -\tilde{x}_2 + \tilde{y}\tilde{x}_1,\\
\frac{\mathrm{d}\tilde{x}_3}{\mathrm{d}t} &= -\tilde{x}_3 + \tilde{y}\tilde{x}_2,\\
\frac{\mathrm{d}\tilde{x}_\nu}{\mathrm{d}t} &= -\tilde{x}_\nu + \tilde{y}\tilde{x}_{\nu-1}, \ \nu = 4,5,6\ldots,\\
\frac{\mathrm{d}\tilde{y}}{\mathrm{d}t} &= \frac{1-\tilde{y}-(\alpha-\tilde{y})\tilde{y}\tilde{x}_2}{1-\tilde{x}_3},
\end{aligned} \tag{2.12}$$

where $\tilde{x}_i$ and $\tilde{y}$ are the dimensionless i-th moment and solute concentration, respectively, and Da and F are dimensionless parameters [6]. On the basis of the system of (2.12), it is clear that the moments of order four and higher do not affect

those of order three and lower, and moreover, the state of the infinite dimensional system:

$$\frac{\mathrm{d}\tilde{x}_\nu}{\mathrm{d}t} = -\tilde{x}_\nu + \tilde{y}\tilde{x}_{\nu-1},\ \nu = 4,\ldots, \tag{2.13}$$

is bounded when x_3 and y are bounded, and it converges to a globally exponentially stable equilibrium point when $\lim_{t\to\infty} x_3 = c_1$ and $\lim_{t\to\infty} \tilde{y} = c_2$, where c_1 and c_2 are constants. This implies that the dominant dynamics (that is, dynamics associated with eigenvalues that are close to the imaginary axis) of the process of (2.1) can be adequately captured by the following fifth-order moment model:

$$\begin{aligned}
\frac{\mathrm{d}\tilde{x}_0}{\mathrm{d}t} &= -\tilde{x}_0 + (1-\tilde{x}_3)Da\mathrm{e}^{-F/\tilde{y}^2},\\
\frac{\mathrm{d}\tilde{x}_1}{\mathrm{d}t} &= -\tilde{x}_1 + \tilde{y}\tilde{x}_0,\\
\frac{\mathrm{d}\tilde{x}_2}{\mathrm{d}t} &= -\tilde{x}_2 + \tilde{y}\tilde{x}_1,\\
\frac{\mathrm{d}\tilde{x}_3}{\mathrm{d}t} &= -\tilde{x}_3 + \tilde{y}\tilde{x}_2,\\
\frac{\mathrm{d}\tilde{y}}{\mathrm{d}t} &= \frac{1-\tilde{y}-(\alpha-\tilde{y})\tilde{y}\tilde{x}_2}{1-\tilde{x}_3}.
\end{aligned} \tag{2.14}$$

The ability of the above fifth-order moment model to reproduce the dynamics, and to some extent the solutions, of the distributed parameter model of (2.1) is shown in Fig. 2.5, where the profiles of the total particle concentration generated by the two models are compared (both models start from the same initial conditions). Even though the discrepancy of the total particle concentration profiles predicted by the two models increases with time (this is expected due to the open-loop instability of the process), it is clear that the fifth-order moment model of (2.14) provides a very good approximation of the distributed parameter model of (2.1), thereby establishing that the dominant dynamics of the system of (2.1) are low dimensional and motivating the use of the moment model for nonlinear controller design.

For the batch crystallization process, the following low-order model can be derived from (2.3) using the method of moments:

$$\begin{aligned}
\frac{\mathrm{d}\mu_0}{\mathrm{d}t} &= \left(1-\frac{4}{3}\pi\mu_3\right)k_2\mathrm{e}^{-\frac{k_3}{(c/c_s-1)^2}}\mathrm{e}^{-\frac{E_b}{RT}},\\
\frac{\mathrm{d}\mu_1}{\mathrm{d}t} &= k_1(c-c_s)\mathrm{e}^{-\frac{E_g}{RT}}\mu_0,\\
\frac{\mathrm{d}\mu_2}{\mathrm{d}t} &= 2k_1(c-c_s)\mathrm{e}^{-\frac{E_g}{RT}}\mu_1,
\end{aligned}$$

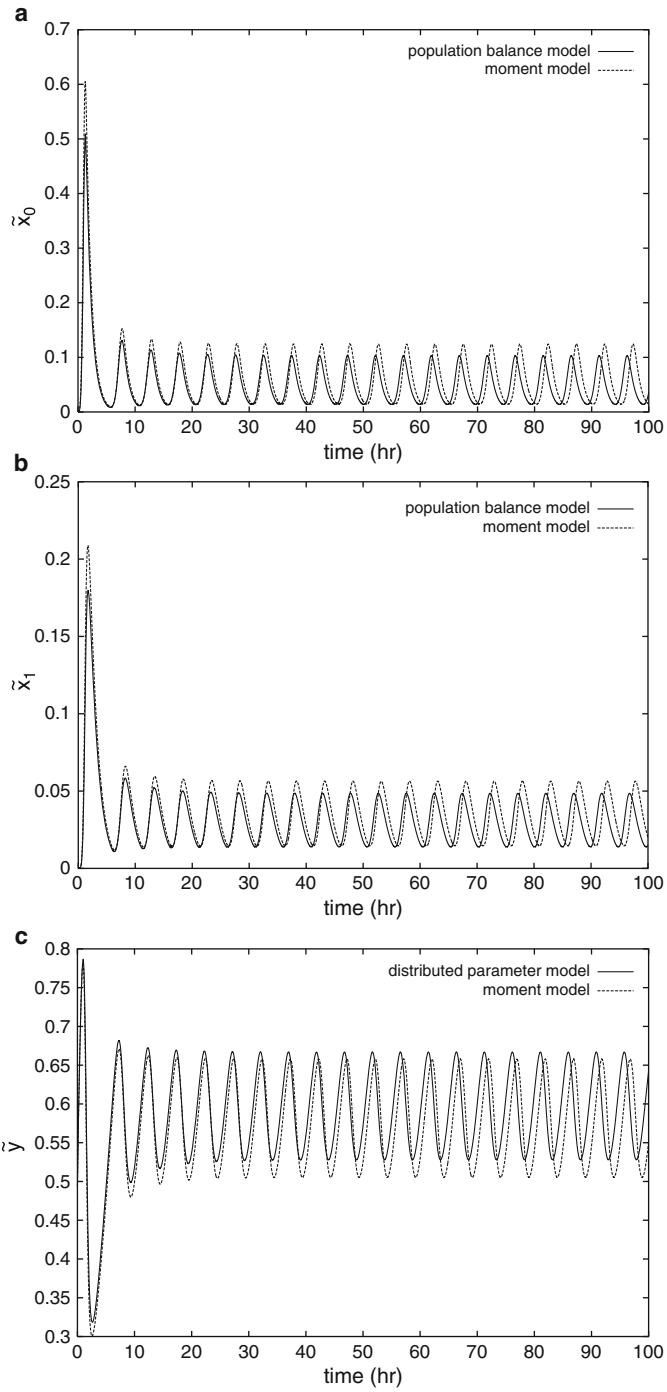

Fig. 2.5 Comparison of open-loop profiles of (**a**) crystal concentration, (**b**) total crystal size, and (**c**) solute concentration obtained from the distributed parameter model and the moment model

$$\begin{aligned}
\frac{\mathrm{d}\mu_3}{\mathrm{d}t} &= 3k_1(c-c_s)\mathrm{e}^{-\frac{E_g}{RT}}\mu_2,\\
\frac{\mathrm{d}c}{\mathrm{d}t} &= \frac{-4\pi(c-c_s)\mu_2(\rho-c)}{\left(1-\frac{4}{3}\pi\mu_3\right)},\\
\frac{\mathrm{d}T}{\mathrm{d}t} &= -\frac{\rho_c\Delta H_c}{\rho C_\mathrm{p}}4\pi k_1(c-c_s)\mathrm{e}^{-\frac{E_g}{RT}}\mu_2 - \frac{UA_c}{\rho C_\mathrm{p}V}(T-T_c),
\end{aligned} \tag{2.15}$$

where E_g and E_b denote the activation energies for growth and nucleation, respectively. The objective is to control the interplay between the particle nucleation and growth rates such that a CSD with a larger average particle size is obtained at the end of the batch run by manipulating the cooling water temperature.

Based on the low-order models, nonlinear finite-dimensional state and output feedback controllers have been synthesized that guarantee stability and enforce output tracking in the closed-loop finite dimensional system. It has also been established that these controllers exponentially stabilize the closed-loop particulate process model. The output feedback controller is constructed through a standard combination of the state feedback controller with a state observer. Specifically, in the case of the continuous crystallization example, the nonlinear output feedback controller has the following form:

$$\begin{aligned}
\frac{\mathrm{d}\omega_0}{\mathrm{d}t} &= -\omega_0 + (1-\omega_3)Da\mathrm{e}^{-F/\omega_4^2} + L_0(\tilde{h}(\tilde{x}) - \tilde{h}(\omega)),\\
\frac{\mathrm{d}\omega_1}{\mathrm{d}t} &= -\omega_1 + \omega_4\omega_0 + L_1(\tilde{h}(\tilde{x}) - \tilde{h}(\omega)),\\
\frac{\mathrm{d}\omega_2}{\mathrm{d}t} &= -\omega_2 + \omega_4\omega_1 + L_2(\tilde{h}(\tilde{x}) - \tilde{h}(\omega)),\\
\frac{\mathrm{d}\omega_3}{\mathrm{d}t} &= -\omega_3 + \omega_4\omega_2 + L_3(\tilde{h}(\tilde{x}) - \tilde{h}(\omega)),\\
\frac{\mathrm{d}\omega_4}{\mathrm{d}t} &= \frac{1-\omega_4-(\alpha-\omega_4)\omega_4\omega_2}{1-\omega_3} + L_4(\tilde{h}(\tilde{x}) - \tilde{h}(\omega))\\
&\quad + \frac{[\beta_2 L_{\tilde{g}}L_{\tilde{f}}\tilde{h}(\omega)]^{-1}\left\{v - \beta_0\tilde{h}(\omega) - \beta_1 L_{\tilde{f}}\tilde{h}(\omega) - \beta_2 L_{\tilde{f}}^2\tilde{h}(\omega)\right\}}{1-\omega_3},\\
\bar{u}(t) &= [\beta_2 L_{\tilde{g}}L_{\tilde{f}}\tilde{h}(\omega)]^{-1}\left\{v - \beta_0\tilde{h}(\omega) - \beta_1 L_{\tilde{f}}\tilde{h}(\omega) - \beta_2 L_{\tilde{f}}^2\tilde{h}(\omega)\right\},
\end{aligned} \tag{2.16}$$

where v is the set-point, β_0, β_1, β_2 and $L = [L_0\ L_1\ L_2\ L_3\ L_4]^T$ are controller parameters and $\tilde{h}(\omega) = \omega_0$ or $\tilde{h}(\omega) = \omega_1$.

The nonlinear controller of (2.16) was also combined with a PI controller (that is, the term $v - \beta_0\tilde{h}(\omega)$ was substituted by $v - \beta_0\tilde{h}(\tilde{x}) + \frac{1}{\tau_i'}\xi$, where $\dot{\xi} = v - \tilde{h}(\tilde{x})$, $\xi(0) = 0$ and τ_i' is the integral time constant) to ensure offsetless tracking in the presence of constant uncertainty in process parameters. The practical implementation of

the nonlinear controller of (2.16) requires online measurements of the controlled outputs $\tilde{x}_0$ or $\tilde{x}_1$; in practice, such measurements can be obtained by using, for example, light scattering [3, 55]. In (2.16), the feedback controller is synthesized via geometric control methods and the state observer is an extended Luenberger-type observer [6].

Several simulations have been performed in the context of the continuous crystallizer process model presented before to evaluate the performance and robustness properties of the nonlinear controllers designed based on the reduced order models, and to compare them with the ones of a PI controller. In all the simulation runs, the initial condition:

$$n(r,0) = 0.0,\, c(0) = 990.0\,\text{kg/m}^3$$

was used for the process model of (2.1) and (2.2) and the finite difference method with 1,000 discretization points was used for its simulation. The crystal concentration, $\tilde{x}_0$, was considered to be the controlled output and the inlet solute concentration was chosen to be the manipulated input. Initially, the set-point tracking capability of the nonlinear controller was evaluated under nominal conditions for a 0.5 increase in the value of the set-point.

Figure 2.6 shows the closed-loop output (left plot) and manipulated input (right plot) profiles obtained by using the nonlinear controller (solid lines). For the sake of comparison, the corresponding profiles under proportional-integral (PI) control are also included (dashed lines); the PI controller was tuned so that the closed-loop output response exhibits the same level of overshoot to the one of the closed-loop output under non-linear control. Clearly, the nonlinear controller drives the controlled output to its new set-point value in a significantly shorter time than the one required by the PI controller, while both controlled outputs exhibit very similar overshoot. For the same simulation run, the evolution of the closed-loop profile and the final steady-state profile of the CSD are shown in Fig. 2.7. An exponentially decaying CSD is obtained at the steady state. The reader may refer to [6] for extensive simulation results.

2.2.4.2 Hybrid Predictive Control

In addition to handling nonlinear behavior, an important control problem is to stabilize the crystallizer at an unstable steady-state (which corresponds to a desired PSD) using constrained control action. Currently, the achievement of high performance, under control and state constraints, relies to a large extent on the use of model predictive control (MPC) policies. In this approach, a model of the process is used to make predictions of the future process evolution and compute control actions, through repeated solution of constrained optimization problems, which ensure that the process state variables satisfy the imposed limitations. However, the ability of the available model predictive controllers to guarantee closed-loop stability and enforce constraint satisfaction is dependent on the assumption of

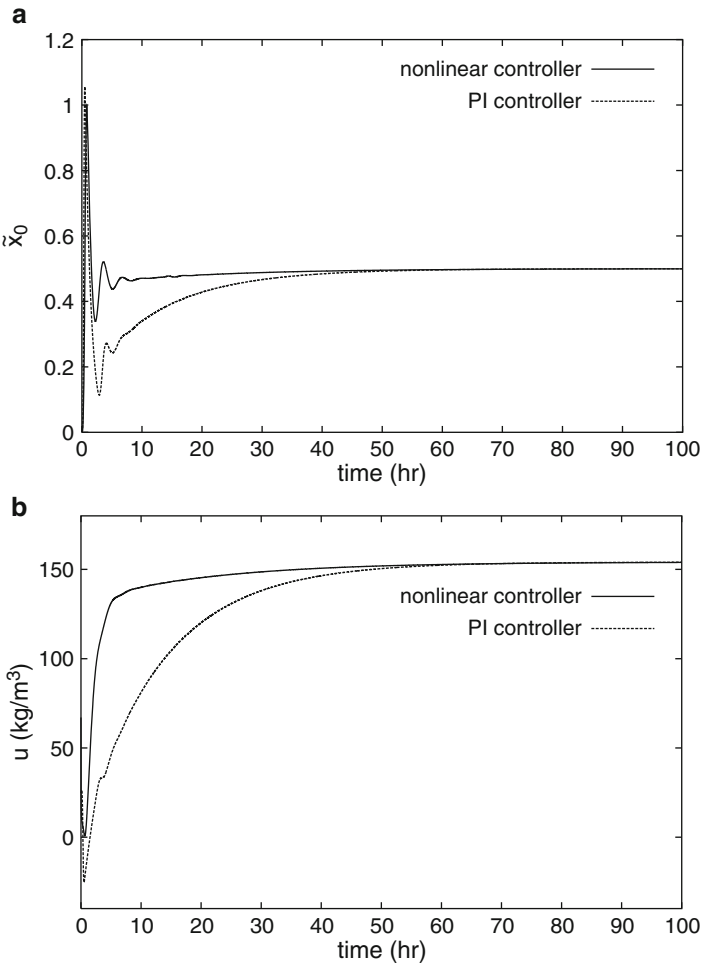

Fig. 2.6 (**a**) Closed-loop output and (**b**) manipulated input profiles under nonlinear and PI control, for a 0.5 increase in the set-point ($\tilde{x}_0$ is the controlled output) [6]

feasibility (i.e., existence of a solution) of the constrained optimization problem. This limitation strongly impacts the practical implementation of the MPC policies and limits the a priori (i.e., before controller implementation) characterization of the set of initial conditions starting from where the constrained optimization problem is feasible and closed-loop stability is guaranteed. This problem typically results in the need for extensive closed-loop simulations and software verification (before online implementation) to search over the whole set of possible initial operating conditions that guarantee stability. This in turn can lead to prolonged periods for plant commissioning. Alternatively, the lack of a priori knowledge of the stabilizing initial conditions may necessitate limiting process operation within a